Journal of Power Sources 233 (2013) 244–251

Contents lists available at SciVerse ScienceDirect

Journal of Power Sources

journal homepage: www.elsevier.com/locate/jpowsour

Significant improvement of electrooxidation performance of carbon in molten carbonates by the introduction of transition metal oxides

Chang Qing Wang, Jia Liu, Jia Zeng, Jin Ling Yin, Gui Ling Wang, Dian Xue Cao*

Key Laboratory of Superlight Material and Surface Technology of Ministry of Education, College of Material Science and Chemical Engineering, Harbin Engineering University, Harbin 150001, China

HIGHLIGHTS

- Graphite electrooxidation activity was remarkably enhanced by transition metal oxides.
- The columbic efficiency of graphite electrooxidation was more than 94%.
- Transition metal oxides reduced the apparent activation energy by 40 kJ mol^{-1}.

ARTICLE INFO

Article history:
Received 6 August 2012
Received in revised form
2 November 2012
Accepted 3 January 2013
Available online 1 February 2013

Keywords:
Carbon electrooxidation
Transition metal oxides
Molten carbonates
Direct carbon fuel cell

ABSTRACT

Solid carbon electrooxidation is the anode reaction of a direct carbon fuel cell. In this study, electrooxidation of graphite in molten carbonates containing transition metal oxides (Fe_2O_3, Co_3O_4, NiO, and MnO_2) is investigated. It is demonstrated that, by dissolving transition metal oxides into the molten Li_2CO_3–K_2CO_3, the onset potential for graphite oxidation is significantly shifted to negative value and the oxidation current density is remarkably increased. At 750 °C, NiO causes a negative shift of onset oxidation potential by around 0.3 V and a current density (at −0.4 V) increase by 4.5 times. The coulombic efficiency of graphite oxidation remains above 94% with and without metal oxides. The apparent activation energy is reduced by more than 40 kJ mol^{-1} by the addition of metal oxides. The working mechanism of the transition metal oxides is interpreted by electronegativity of metal cations, the concentration of oxygen anions and the indirect oxidation pathway via preceding chemical reaction-following electrochemical reaction.

1. Introduction

Coal is the most abundant and economic fossil fuel on earth and accounts for 27% of the world's primary energy consumption nowadays. This number is forecasted to remain through 2035, implying that coal will still be one of the primary energy source in the near future [1]. Unlike petroleum, most of coal reserves still remain underused. The critical issues for the use of coal for power generation in the conventional coal-fired plants include the low efficiency determined by the thermal engines and the release of significant amount of environmentally harmful gases (e.g., CO_x, NO_x and SO_x) and particulates. Therefore, seeking new technologies for the conversion of coal to electricity efficiently and cleanly becomes very important to meet needs for clean energy production and sustainable energy supply. This is especially true for those countries largely relying on coal for power production, such as, China, around 80% of its electricity was generated in coal-fired power plants [1]. The direct carbon fuel cell (DCFC), which allows the direct conversion of the chemical energy of solid carbon materials into electricity via an electrochemical route instead of the direct combustion, provides a promising means for the conversion of coal to electricity in an efficient and clean way [2–5].

DCFC shares the same electrochemical principle as conventional fuel cells. In its anode, carbon is electrochemically oxidized to CO_2 releasing 4 electrons; in the cathode, oxygen from air combines with these electrons and is electrochemically reduced. The electrical power is generated based on the overall reaction of $C + O_2 = CO_2$ [2,3,5]. The uniqueness of DCFC is that it relies on a solid carbonaceous material as its fuel. Unlike other fuels (such as hydrogen, methane, and alcohol), solid carbon fuels are cheap, abundant and readily available. They can be coal, coke, graphite, biomass (such as rice hulls, nut shells, corn husks, grass, and woods), and municipal solid wastes. Besides, compared with hydrogen fuel cells and coal-fired power plants, DCFC has other

* Corresponding author. Tel./fax: +86 451 82589036.
E-mail address: caodianxue@hrbeu.edu.cn (D.X. Cao).

0378-7753/$ – see front matter © 2013 Elsevier B.V. All rights reserved.
http://dx.doi.org/10.1016/j.jpowsour.2013.01.016

advantages [2,3,5]: (1) DCFC has a theoretical electrochemical efficiency ($\Delta G/\Delta H$) of nearly 100% due to the near-zero entropy change of the cell reaction at high temperature. A practical efficiency of around 80% has been demonstrated. (2) The fuel utilization in a DCFC system can reach up to 100% because the reaction product, CO_2, exists in a separate gas phase and thus does not influence the activity (chemical potentials) of the solid carbon. (3) DCFC has lower emissions than conventional coal-fired power plants since, in principle, the anodic off gas of a DCFC is almost pure carbon dioxide, which can be captured and sequestered with less difficulty than that from conventional thermal power plants. (4) DCFC can be integrated with hydrogen fuel cell and/or concentrated solar power reactor to significantly increase the energy conversion efficiency of hydrocarbon-based power generation systems [6,7]. So DCFC, a century-old technology, re-attracted significant research interests in recent years [8–51].

In order to generate practically useable power output, DCFC has to be operated at elevated temperature (i.e., higher than 650 °C) using molten carbonate and/or solid oxide as electrolytes to overcome the sluggish kinetics of electrochemical oxidation of solid carbon in the anode. Therefore, improving the electrooxidation activity of solid carbon in molten salts becomes a key issue for the enhancement of DCFC performance and the lowering of its operation temperature. Decreasing the working temperature will effectively restrict the reverse Boudouard reaction (Eq. (1)), which is thermodynamically favored at temperatures above 700 °C [5].

$$C + CO_2 = 2CO \quad (1)$$

This side reaction leads to decrease of carbon fuel utilization efficiency. In addition, DCFC, operating at low temperature, allows the use of low cost fuel cell materials. Several efforts have been made in different aspects to increase the electrooxidation activity of solid carbon in molten carbonates, which include: the surface modification of carbon fuels [31,52,53], the use of catalysts [14,15,33] and the preparation of highly active carbons [54–56]. For example, results from Li et al. [52,53] and our group [31] showed that the electrochemical reactivity of activated carbon are significantly improved by surface treatments with strong acids (e.g., HNO_3, HCl, HF). Nabae et al. [33] found that carbon black, when impregnated with Ni, exhibits obviously enhanced electrooxidation kinetics.

In this work, we reported a feasible, economic and practically applicable way to improve the electrochemical oxidation activity of carbon in molten carbonates. We demonstrated that by simply adding a small amount of transition metal oxides to the molten carbonate electrolytes, the electrooxidation performance of carbon was remarkably enhanced. The promotion mechanism of metal oxides to carbon electrooxidation was discussed.

2. Experimental

Electrooxidation of carbon in molten salts was carried out in a specially designed 3-electrode electrochemical cell (Fig. 1). A high purity graphite rod (purity >99.99%) with a diameter of 6 mm was used as the working electrode (also the reactant). The graphite rod was tightly inserted into an alumina tube with only 10 mm in length exposed and contacted with the electrolyte. So the initial reaction area was fixed at around 1.884 cm^2 (the current density was normalized to this area). The reference electrode was an Au/CO_3^{2-}/O_2,2CO_2 electrode, which was constructed from a closed-bottom alumina tube (with a pin hole) containing a gold wire and an overflow mixture gas of 33%O_2–67% CO_2 (by volume). The gold wire was polished with sand paper, etched in 50% HCl for 30 s, and rinsed with distilled water prior to each run. The container of the electrochemical cell was made of 316 stainless steel; it also served as the counter electrode. The cell was equipped with two alumina tubes for gas feeding and exiting, respectively. N_2 gas flowed through the cell to keep the reaction system free from air and to remove CO_2 generated during measurements. The current-potential polarization curves and the chronoamperometric curves were measures using a computerized VMP3/Z potentiostat (Bio-logic) controlled by the EC-lab software. For the cyclic voltammetric measurements of metal oxides in molten carbonates, a Au wire and a pieces of Au sheet was used as the working and counter electrode, respectively, and an alumina crucible was used as the cell container. All potentials were referred to the Au reference electrode.

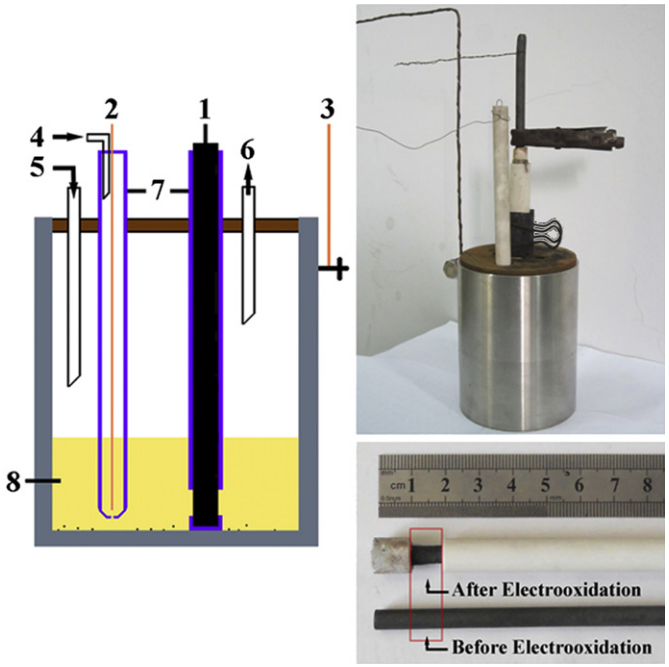

Fig. 1. The schematic diagram of the three-electrode electrochemical cell (left). Photographs of the experimental setup and the graphite rod working electrode before and after electrooxidation (right).

The base electrolyte was the mixture of 38 g Li_2CO_3 and 62 g K_2CO_3. To investigate the promotion effects of metal oxides (Fe_2O_3, Co_3O_4, MnO_2, and NiO) in the molten carbonate electrolyte on the electrooxidation of graphite, metal oxides was added to the mixture of carbonates by finely grounding the dried metal oxides powers with the carbonates power. The obtained mixtures were put into the cell at room temperature and then heated by a crucible furnace to the required reaction temperatures with the protection of nitrogen gas flow. After measurements, the molten mixtures were sampled and the contents of metal oxides dissolved in the molten carbonates were analyzed using inductive coupled plasma emission spectrometer (ICP, Xseries II, Thermo Scientific).

The off-gas compositions of graphite electrooxidation were analyzed by a gas chromatograph (Agilent GC 6890) using a PLOT U column and nitrogen carrier gas. To collect the gas samples, the electrochemical cell was first purged with ultrahigh purity nitrogen and then sealed. A long stainless syringe needle was implanted to the airtight cell and it was connected to a glass syringe for the collection of gas products.

3. Results and discussion

3.1. Dissolution of metal oxides in molten carbonates

0.1 g of transition metal oxides (Fe_2O_3, Co_3O_4, NiO, MnO_2) were mixed with 38 g Li_2CO_3 and 62 g K_2CO_3 to make sure the molten

carbonates were saturated with the dissolved metal oxides. Table 1 listed the solubility of metal oxides in the molten carbonates measure by ICP analysis. The concentrations of metal ions and O^{2-} were also calculated assuming that the dissolved metal oxides are completely dissociated into their respective cations and anions based on the fact that they are highly dissociated. As seen, the solubility of the transition metal oxides is in the order of 10^{-4} mol per 100 g carbonates (i.e., 32 g Li_2CO_3 + 68 g K_2CO_3). The solubility of NiO and Fe_2O_3 is in good agreement with that reported in literature [57,58].

3.2. Effects of transition metal oxides on the electrooxidation of graphite

Electrooxidation of graphite was investigated by linear potential sweep at a scan rate of 2 mV s^{-1} starting from the open circuit potential (OCP). The electrode was stabilized at the OCP for 10 min prior to the measurements. The reaction temperature was between 650 and 850 °C with a 50 °C increment. Fig. 2 shows the typical voltammetric curves without and with metal oxides at 750 °C (see Supporting information for the curves at other temperatures). First, the onset potential for graphite electrooxidation was significantly shifted to more negative potential with the addition of metal oxides, for example, from −0.60 V in Li_2CO_3–K_2CO_3 to −0.89 V in Li_2CO_3–K_2CO_3–NiO. Secondly, in the whole potential range, the oxidation current density in the presence of metal oxides is much higher than that in the absence of metal oxides. For example, at −0.4 V, the current density is 17 mA cm^{-2} in Li_2CO_3–K_2CO_3, but 117 mA cm^{-2} in Li_2CO_3–K_2CO_3–NiO. These observations clearly indicated that the addition of metal oxides enhanced the performance of graphite electrooxidation both thermodynamically and kinetically.

In order to examine the effect of metal oxides on the electrooxidation performance of graphite at different reaction temperatures, the OCP and the current density at −0.4 V (taken from the voltammetric curves) were plotted against temperature for different metal oxides; and the results are shown in Fig. 3 and Fig. 4, respectively. Fig. 3 shows the dependence of OCP on temperature for different metal oxides. As can be seen that, the OCP depends upon both the metal oxides and the reaction temperature. At temperatures below 800 °C, all the metal oxides caused significant negative shift of OCP, and the shift is more remarkable at lower temperatures (i.e., below 750 °C), which indicated that the pronounced enhancement of graphite electrooxidation performance mainly occurred at low reaction temperatures. At 850 °C, the addition of Fe_2O_3 and Co_3O_4 increases the OCP slightly. NiO and MnO_2 are more effective for the reduction of OCP than Fe_2O_3 followed by Co_3O_4, particularly at temperatures higher than 750 °C. While, at 650 °C, all the metal oxides perform similarly and caused a negative shift of OCP by around 0.2 V. The largest negative shift of OCP was 0.3 V, which occurred at 750 °C in the Li_2CO_3–K_2CO_3–NiO electrolyte. The significant negative shift of OCP is very important

Table 1
The solubility of transition metal oxides and the concentrations of their respective cations and anions in 750 °C molten Li_2CO_3–K_2CO_3.

Metal oxides	Concentration of metal oxides (mol per 100 g[b])	Concentration of metal ions (mol per 100 g)[a]	Concentration of O^{2-} (mol per 100 g)[a]
Fe_2O_3	2.4×10^{-4}	4.8×10^{-4}	7.2×10^{-4}
Co_3O_4	1.9×10^{-4}	5.7×10^{-4}	7.6×10^{-4}
NiO	1.01×10^{-4}	1.01×10^{-4}	1.01×10^{-4}
MnO_2	8.55×10^{-4}	8.55×10^{-4}	1.71×10^{-3}

[a] Assuming complete dissociation of metal oxides.
[b] 100 g means 32 g Li_2CO_3 + 68 g K_2CO_3.

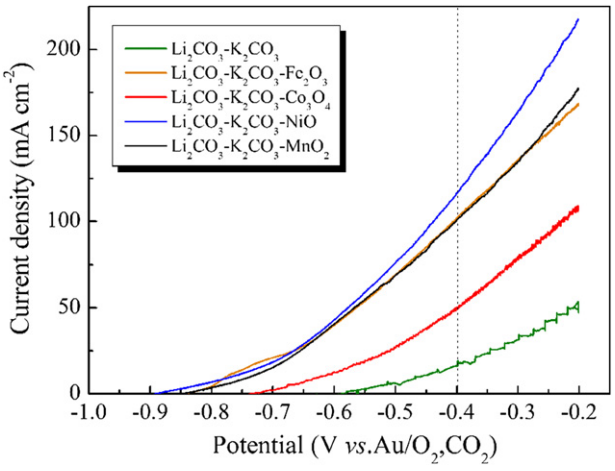

Fig. 2. Polarization curves of graphite electrode measured in 750 °C molten Li_2CO_3–K_2CO_3 without and with transition metal oxides at a scan rate of 2 mV s^{-1}.

because it means the increase of the open circuit voltage of DCFC, i.e., the increase in the maximum reachable voltage efficiency of DCFC ($\eta_V = V_{OCP}/V_{theoretical}$, $V_{theoretical}$ = 1.02 V). So based on our results, the maximum reachable voltage efficiency of DCFC using graphite as fuel and molten Li_2CO_3–K_2CO_3 as electrolyte is around 60% at 750 °C. However, when NiO was introduced to the Li_2CO_3–K_2CO_3 electrolyte, the efficiency reached 89%.

Fig. 4 shows the dependence of the current density at −0.4 V on temperature for different transition metal oxides. Clearly, the current densities for graphite electrooxidation in molten Li_2CO_3–K_2CO_3 containing Fe_2O_3 or MnO_2 or NiO were significantly higher than that in pure Li_2CO_3–K_2CO_3 at all the temperatures investigated. Co_3O_4 performs slightly differently. With and without Co_3O_4, the current density at 850 °C is the same, but at other temperatures, the presence of Co_3O_4 still increased the current density. More specifically, at temperatures below 750 °C, the current density for graphite electrooxidation in molten Li_2CO_3–K_2CO_3 containing saturated Fe_2O_3, MnO_2 and NiO is more than 4, 3 and 5 times of that without metal oxides respectively. This value is around 2 at temperatures higher than 750 °C. So the effect of metal oxides on the electrooxidation rate of graphite is more remarkable at lower temperature. This means that the working temperature of DCFC can be decreased by the addition of transition metal oxides in

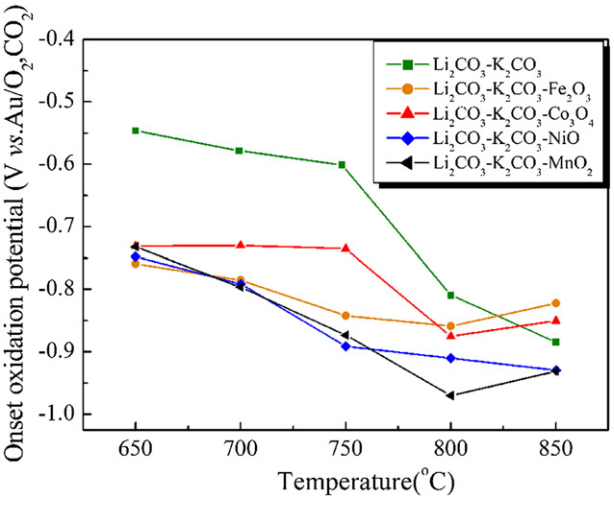

Fig. 3. Dependence of onset potential for graphite oxidation on temperature.

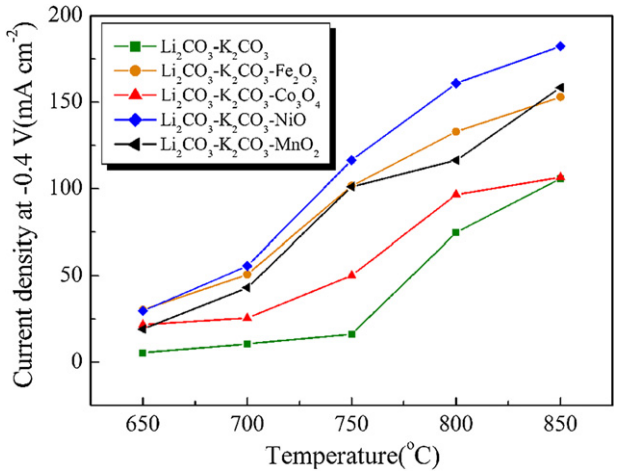

Fig. 4. Dependence of current density at −0.4 V for graphite oxidation on temperature.

the molten Li_2CO_3–K_2CO_3 electrolyte. The decrease of DCFC operation temperature will enhance the carbon conversion and utilization efficiency by limiting the reverse Boudouard reaction, and will relax the requirement of fuel cell materials. As far as we know, such significant improvement in electrooxidation activity of carbon has not been reported.

The stabilities of graphite electrooxidation in Li_2CO_3–K_2CO_3 without and with metal oxides were investigated by constant potential discharge experiments. Fig. 5 shows the chronoamperometric curves at −0.4 V and 750 °C. As can be seen, the current densities for graphite electrooxidation in Li_2CO_3–K_2CO_3 and Li_2CO_3–K_2CO_3 containing Fe_2O_3 or MnO_2 or NiO are nearly constant within the 30 min test period. The current density in Li_2CO_3–K_2CO_3–Co_3O_4 slightly increased in the first 10 min and then stabilized. So the results demonstrated that the enhanced reaction rates of graphite by the addition of metal oxides in Li_2CO_3–K_2CO_3 are sustainable. The current density at the end of tests was 28 mA cm^{-2} in the absence of metal oxides, and was 46, 83, 100, and 126 mA cm^{-2} in the presence of Co_3O_4 Fe_2O_3, MnO_2, or NiO, respectively. The promotion effect of metal oxides on the electrooxidation activity of graphite is in the order of NiO > MnO_2 > Fe_2O_3 > Co_3O_4.

3.3. Gaseous products and coulombic efficiency

Electrooxidation of carbon in molten carbonates can be represented by the following two equations (Eq. (2) and Eq. (3)) [2,59].

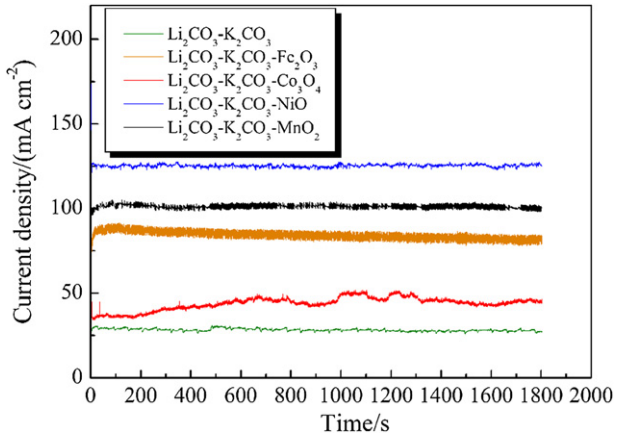

Fig. 5. Chronoamperometric curves for graphite electrooxidation at −0.4 V and 750 °C.

The reverse Boudouard reaction (Eq. (1)) can be seen as a linear combination of these two reactions.

$$C + 2CO_3^{2-} \rightarrow 3CO_2 + 4e^- \quad (2)$$

$$C + CO_3^{2-} \rightarrow CO_2 + CO + 2e^- \quad (3)$$

Eq. (2) is the ideal one because via which carbon was completely electrooxidized with the release of total four electrons. Eq. (3) (also the reverse Boudouard reaction) is the incomplete electrooxidation of carbon leading to the formation of CO and the release of only two electrons, which implies low utilization efficiency of carbon fuel. Cooper and Selman [2] suggested that the coulombic efficiency of carbon electrooxidation in molten carbonates can be determined using Eq. (4) by the analysis of relative composition of CO and CO_2 in the off-gas.

$$\eta = \frac{x+2}{2(2x+1)} \quad (4)$$

where $x = [CO]/[CO_2]$. Accordingly, the coulombic efficiency would be 100% if the carbon oxidation proceeds via Eq. (2), and 67% if goes by Eq. (3) (and the reverse Boudouard reaction).

In order to examine whether the addition of metal oxides to the Li_2CO_3–K_2CO_3 affect the coulombic efficiency of graphite electrooxidation, we analyzed the ratio of CO to CO_2 in the gaseous products and calculated the coulombic efficiency using Eq. (4). Table 2 shows the coulombic efficiency of graphite electrooxidation in Li_2CO_3–K_2CO_3 without and with MnO_2 at different potentials and temperatures. Obviously, the addition of MnO_2 to the Li_2CO_3–K_2CO_3 did not alter the coulombic efficiency, and the effects of temperature and potential on the coulombic efficiency are also insignificant. The coulombic efficiency remains higher than 94% in Li_2CO_3–K_2CO_3 without and with MnO_2 at temperatures ranging from 650 to 850 °C and potentials between −0.4 V and −0.2 V. This result is in good agreement with that reported by Hauser [60], who found that the anodic oxidation of graphite rods predominately generates CO_2 at the current density of 50–100 mA cm^{-2} and coulombic efficiencies are more than 95% in the temperature range of 650–800 °C. However, as pointed out by Cooper [2], the sluggish kinetics of electrooxidation of the dense and highly ordered graphite in conventional molten carbonates electrolytes severely limited power output and therefore practical applications. However, this study demonstrated that the fast electrooxidation of graphite with high coulombic efficiency is achievable by saturating molten Li_2CO_3–K_2CO_3 with transition metal oxides. Notably, highly disordered carbons usually displayed higher electrooxidation activity than graphite, so it is expected that the electrooxidation performance of amorphous carbons (e.g. carbons from coal and biomass) might be even more remarkably improved by the addition of transition metal oxides in the molten Li_2CO_3–K_2CO_3 electrolyte than that of graphite. Such investigations are undergoing in our

Table 2
Columbic efficiency of graphite electrooxidation in molten Li_2CO_3–K_2CO_3 without and with MnO_2.

T/°C	$Li_2CO_3 + K_2CO_3$				$Li_2CO_3 + K_2CO_3 + MnO_2$			
	−0.4 V		−0.2 V		−0.4 V		−0.2 V	
	CO/CO_2	η	CO/CO_2	η	CO/CO_2	η	CO/CO_2	η
650	0.043	94.1%	0.023	96.7%	0.038	94.7%	0.036	95.0%
700	0.039	94.6%	0.04	94.4%	0.041	94.3	0.041	94.3%
750	0.025	96.4%	0.016	97.7%	0.031	95.6%	0.021	97.0%
800	0.018	97.4%	0.015	97.8%	0.02	97.1%	0.015	97.8%
850	0.013	98.1%	0.0095	98.6%	0.017	97.5%	0.011	98.4%

laboratory. In this study, we chose graphite rod, instead of particulate carbon, as the working electrode. This is because graphite rod served as both the reactant (fuel) and the current collector (Fig. 1), which ensures the obtained data to be reliable. If particulate carbon is used as the fuel, an additional current collector is needed for forming the working electrode, and the contact between the current collector and carbon particulates is usually less controllable, which results in poor reproducibility of the experimental dada.

3.4. Role of metal oxides

Investigation of the electrooxidation mechanism of solid carbon in high temperature molten salts is quite difficult because conventional analysis techniques are hardly applicable to such a system. This is the reason why publications on the mechanism study are so rare. In this study, the working mechanism of transition metal oxides was explained based on some fundamental data and principles. Three reasons are possibly responsible for the significant enhancement of graphite electrooxidation activity caused by the addition of transition metal oxides in the molten Li_2CO_3–K_2CO_3, which are discussed below.

Cooper et al. suggested a mechanism for the anodic oxidation of carbon in molten carbonates (Eqs. (5)–(13) [2,48]. The reaction was initiated by the dissociation of carbonate to form a free oxide ion (Eq. (5)), which adsorbs on the carbon surface and is discharged in two, one-electron steps to form a strongly bound CO functional group at reactive carbon sites (C_s) Eqs. (6)–(8). This CO group decomposes very slowly to form CO (Eq. (9)). The second O^{2-} adsorbs to -CsCO sites (Eq. (10)). The resulted species undergoes subsequent discharge in two, one-electron transfer steps to form an unstable group, C_sCO_2 Eqs. (11) and (12), which is readily desorbed as CO_2 (Eq. (13)).

The first five steps Eqs. (5)–(9) have the net overall reaction of Eq. (3), which corresponds to a two-electron transfer process leading to the formation of a mixture of CO and CO_2. If the reaction sequence continues without the dissociation of CO (Eq. (9)) until the final step, then the four electron transfer occurs according to Eq. (2) resulting in the formation of pure CO_2.

$$CO_3^{2-} \rightarrow CO_2 + O^{2-} \quad \text{Carbonate dissociation} \tag{5}$$

$$C_SC + O^{2-} \rightarrow C_SCO^{2-} \quad 1^{st}\ O^{2-}\ \text{adsorption} \tag{6}$$

$$C_SCO^{2-} \rightarrow C_SCO^{-} + e^{-} \quad 1^{st}\ \text{electron discharge} \tag{7}$$

$$C_SCO^{-} \rightarrow C_SCO + e^{-} \quad 2^{nd}\ \text{electron Fast discharge} \tag{8}$$

$$C_SCO \rightarrow C_S + CO \quad \text{CO desorption} \tag{9}$$

$$C_SCO + O^{2-} \rightarrow C_SCO_2^{2-} \quad 2^{nd}\ O^{2-}\ \text{adsorption (RDS)} \tag{10}$$

$$C_SCO_2^{2-} \rightarrow C_SCO_2^{-} + e^{-} \quad 3^{rd}\ \text{electron discharge} \tag{11}$$

$$C_SCO_2^{-} \rightarrow C_SCO_2 + e^{-} \quad 4^{th}\ \text{electron discharge} \tag{12}$$

$$C_SCO_2 \rightarrow C_S + CO_2 \quad CO_2\ \text{desorption} \tag{13}$$

The step involving the adsorption of the second O^{2-} adjacent to -CsCO sites (Eq. (10)) is assumed to be the rate determining step (RDS). This is because the -CsCO sites are electronegative, the adsorption of negatively charged O^{2-} to these sites is severely hindered by charge repulsion, and therefore requires considerable additional energy input (overpotential). Accordingly, if the electronegative degree of the -CsCO sites can be reduced, the adsorption of O^{2-} adjacent to it will become easier, and thus the energy barrier of the RDE can be lowered. Consequently, the overall rate of carbon electrooxidation (Eq. (4), four electron process) can be enhanced. Table 3 lists the electronegativity of metal cations possibly existing in the electrolyte [61,62]. Coincidentally, the transition metal cations have larger electronegativity than Li^+ and K^+ (more than 1.5 times), meaning that they have stronger ability to withdraw negative charge than Li^+ and K^+. Therefore, we proposed that transition metal cations might adsorb adjacent to the electronegative -CsCO sites and pull the electrons away from these sites (as illustrated in Fig. 6). So the -CsCO sites become less electronegative and the adsorption of O^{2-} requires less additional energy. To support this assumption, we determined the apparent activation energy E_a by plotting the logarithm of current density at −0.4 V as a function of the reciprocal of absolute temperature (Fig. 7). The slope of a linear fit gives the E_a based on the Arrhenius equation. E_a is 217 kJ mol^{-1} in Li_2CO_3–K_2CO_3, and 74, 79, 82, and 92 kJ mol^{-1} in Li_2CO_3–K_2CO_3 with dissolved Fe_2O_3, Co_3O_4, NiO, and MnO_2, respectively. Apparently, transition metal oxides reduced the activation energy of carbon electrooxidation. So in this respect, transition metal oxides behave like catalysts.

In order to overcome the slow kinetics of the direct electrochemical oxidation of carbon, an alternative strategy, named indirect electrooxidation of carbon, was investigated. That is, a secondary redox system (couples of transition metal ions) was introduced into the carbon anode compartment, in which metal ions were reduced by carbon chemically and then re-oxidized and renewed at the anode electrochemically [63]. So the redox couple served as a mediator to catalyze the electrooxidation of carbon indirectly. This idea is based on the fact that several transition metal ions, including Fe^{3+}, Sn^{4+}, Cu^{2+}, and Ce^{4+}, can oxidize coal slurries with activation energy significantly lower than that for the direct electrooxidation of coal. This concept has also been adopted to solve another problem of DCFC, that is, Eq. (2) requires transfer of electrons so that a metallic current collector must be incorporated into the anode structure (carbon slurry) and only those carbon particles, which are in contact with the current collector (directly or indirectly), can be electrooxidized. Thus, the region for Eq. (2) to occur is limited, and so the performance of DCFC. In this case, molten metals (e.g. Sn, Sb, Pb, Bi, In) instead of metal ions were used as the mediate redox system [18,27,50,64]. The molten metals can be electrooxidized at the anode generating molten metal oxides, which were then reduced by carbon. As a result, carbon was indirectly oxidized to generate electricity. Several recent studies have demonstrated that this concept of indirect oxidation of carbon via a redox couple (mediator) works quite well [18,50,63,64]. In this work, the transition metal oxides dissolved in Li_2CO_3–K_2CO_3 might also serve as a mediator to bridge the indirect electrooxidation of carbon, as represented by Eqs. (14) and (15) (where $x > y$), as well as

Table 3
Electronegativity of transition metal cations [61,62].

Metal cation	Electronegativity
K^+	0.897
Li^+	0.943
Fe^{2+}	1.438
Fe^{3+}	1.687
Co^{2+}	1.467
Co^{3+}	1.754
Ni^{2+}	1.502
Ni^{3+}	1.786
Mn^{2+}	1.426
Mn^{4+}	1.953

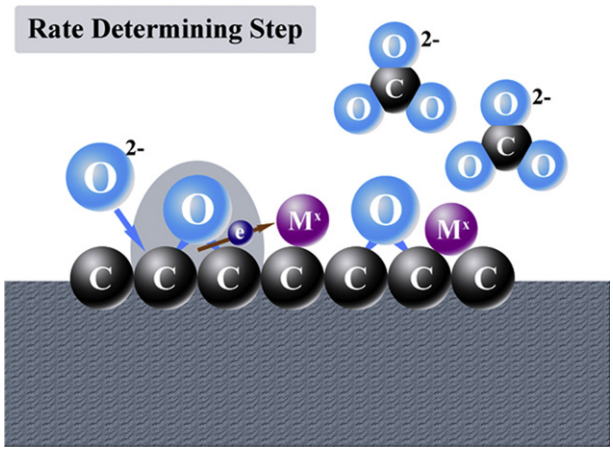

Fig. 6. Schematic representation of the rate determining step (Eq. (10)) of carbon electrooxidation in molten Li_2CO_3–K_2CO_3 containing transition metal oxides which shows the pulling away of negative charge by positive metal ions.

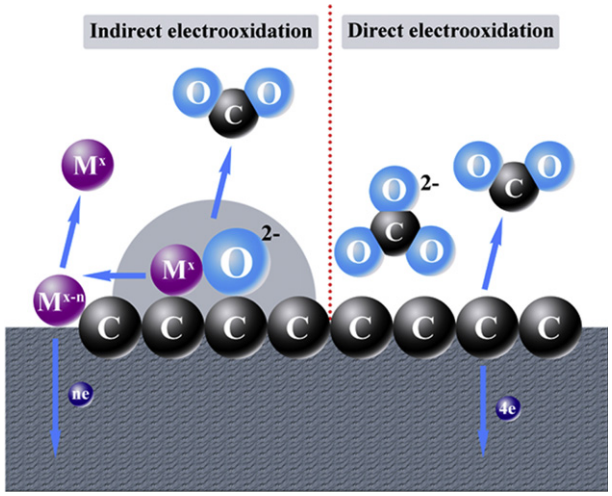

Fig. 8. Schematic representation of the indirect and direct pathways for carbon electrooxidation in molten Li_2CO_3–K_2CO_3 containing transition metal oxides.

illustrated in Fig. 8. That is, graphite was first oxidized by metal oxides chemically (Eq. (14)). The reduced metal oxides were then electrochemically re-oxidized (Eq. (15)). This is the so called CE mechanism, that is, the overall reaction is composed of a chemical reaction followed by an electrochemical reaction. The net reaction is the four electron electrooxidation of carbon.

$$\frac{4}{x-y}M^x + 2O^{2-} + C \rightarrow CO_2 + \frac{4}{x-y}M^y \quad \text{Preceding chemical reaction} \tag{14}$$

$$\frac{4}{x-y}M^x \rightarrow \frac{4}{x-y}M^y + 4e^- \quad \text{Following electrochemical reaction} \tag{15}$$

This mechanism works only if Eq. (14) is thermodynamically favored. Furthermore, Table 4 listed our calculated Gibbs free energies for Eq. (14) with M = Fe, Co, Ni and Mn. As can be seen that, all these chemical reactions have negative Gibbs free energies and are therefore spontaneous. On the other hand, from the point view of electrochemistry, for Eq. (14) to be spontaneous, the reduction potential of Eq. (15) must be higher than the oxidation potential of carbon. Fig. 9 shows the cyclic voltammograms (CV) of Au electrode in molten Li_2CO_3–K_2CO_3 without and with the dissolved transition metal oxides. The CV only shows double layer currents in molten Li_2CO_3–K_2CO_3 in the potential range of around −0.9 to −0.2 V. Significantly higher cathodic and anodic currents than the double layer currents were observed in molten Li_2CO_3–K_2CO_3 containing MnO_2 or NiO. So these currents must come from the redox reaction of metal oxides. Licht et al. [65] and Yin et al. [66] reported a similar CV for Fe_2O_3 in molten carbonates and they attributed the oxidation–reduction peak to the transformation of Fe^{2+}/Fe^{3+}. The onset reduction potential of MnO_2 and NiO roughly estimated for their CV is around −0.3 V, which are higher than the onset potential for graphite electrooxidation (−0.6 V as shown in Fig. 3). This indicated that Reaction (14) can take place thermodynamically [64]. It should be pointed that the indirect and direct electrooxidation of graphite should occur simultaneously (Fig. 8).

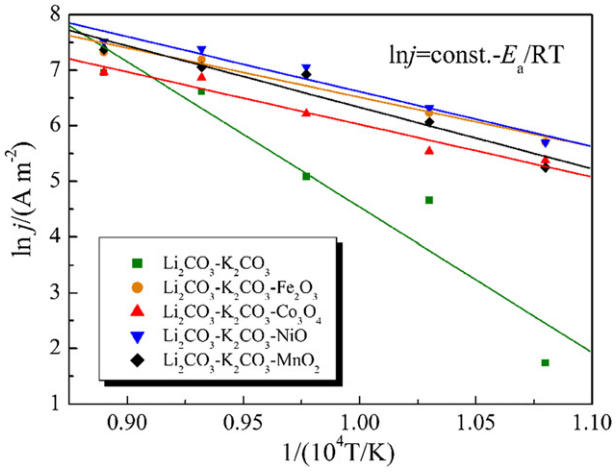

Fig. 7. Arrhenius plots of the current density at −0.4 V against temperature.

Finally, the concentration of O^{2-} might also affect the performance of graphite electrooxidation. According to the oxidation mechanism of carbon proposed by Cooper et al. Eqs. (5)–(13), the oxidation of carbon was initiated by the adsorption of first O^{2-}(Eq. (6)) and the rate was determined by the adsorption of second O^{2-}(Eq. (10)). So the increase of O^{2-} concentration is expected to increase the rate of carbon electrooxidation. In molten Li_2CO_3–K_2CO_3, the O^{2-} comes from the dissociation of CO_3^{2-} (eq. (5)) and its concentration is $\sim 10^{-4}$ mol per 32 g Li_2CO_3 + 68 g K_2CO_3 [48]. As seen from Table 1, assuming all the dissolved metal oxides were completely dissociated to metal ions and O^{2-}, then the concentration of O^{2-} would be at least doubled by the addition of metal oxides to the Li_2CO_3–K_2CO_3. So metal oxides might also act as the sources of O^{2-}.

At this stage, it is hard to distinguish which of the above mechanism is more (or solely) responsible for the remarkable improvement of carbon electrooxidation activity. It is most likely that all these mechanisms work simultaneously to some extent.

Table 4
Gibbs free energy of chemical reactions between carbon and transition metal oxides.

Chemical reaction	Gibbs free energy (kJ mol^{-1})
$C + 2Fe_2O_3 = CO_2 + 4FeO$	−3337.11
$C + 2Co_3O_4 = CO_2 + 6CoO$	−278.50
$C + 2NiO = CO_2 + 2Ni$	−56.15
$C + 2MnO_2 = CO_2 + 2MnO$	−289.79

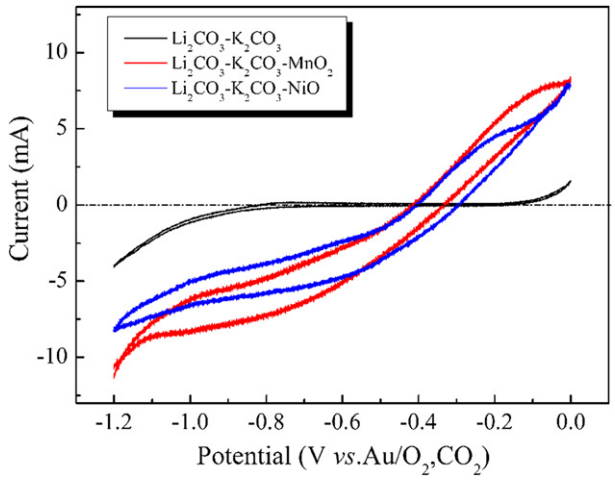

Fig. 9. Cyclic voltammograms in 750 °C molten $Li_2CO_3K_2CO_3$ without and with dissolved NiO or MnO_2 at a scan rate of 2 mV s^{-1}.

4. Conclusions

The electrooxidation performance of graphite in molten carbonates was remarkably enhanced kinetically and thermodynamically by simply saturating the molten electrolyte with transition metal oxides, such as Fe_2O_3, Co_3O_4, NiO, and MnO_2. More significant performance enhancement was observed at low reaction temperatures. The oxidation current density of graphite in molten Li_2CO_3–K_2CO_3 was increased by more than 7 times with the addition of NiO in the electrolyte at 750 °C. The effectiveness of metal oxides for the enhancement of graphite electrooxidation performance is of the order NiO > MnO_2 > Fe_2O_3 > Co_3O_4. The operation temperature of DCFC can be effectively reduced by the introduction of small amount of transition metal oxides. The effects of transition metal oxide were correlated with the electronegativity of metal cations and the concentration of oxygen anions. An indirect electrooxidation pathway was also proposed to explain the activity improvement.

Acknowledgments

We gratefully acknowledge the financial support of this research by National Nature Science Foundation of China, the Fundamental Research Funds for the Central Universities (HEUCFT1205), Harbin Science and Technology Innovation Fund for Excellent Academic Leaders (2012RFXXG103), and Specialized Research Fund for the Doctoral Program of Higher Education (20102304110001).

Appendix A. Supplementary data

Supplementary data related to this article can be found at http://dx.doi.org/10.1016/j.jpowsour.2013.01.016.

References

[1] International Energy Outlook, Report Number: DOE/EIA-0484(2011), available at: http://www.eia.doe.gov/oiaf/ieo/coal.html.
[2] J.F. Cooper, R. Selman, ECS Trans. 19 (2009) 15–25.
[3] D. Cao, Y. Sun, G. Wang, J. Power Sources 167 (2007) 250–257.
[4] A.L. Dicks, J. Power Sources 156 (2006) 128–141.
[5] P. Desclaux, S. Nürnberger, U. Stimming, in: R. Steinberger-Wilckens, W. Lehnert (Eds.), Innovations in Fuel Cell Technologies, The Royal Society of Chemistry, 2010, pp. 190–210.
[6] G. Cinti, K. Hemmes, Int. J. Hydrogen Energy 36 (2011) 10198–10208.
[7] N. Muradov, P. Choi, F. Smith, G. Bokerman, J. Power Sources 195 (2010) 1112–1121.
[8] J. Zhang, Z. Zhong, D. Shen, J. Xiao, Z. Fu, H. Zhang, J. Zhao, W. Li, M. Yang, J. Power Sources 196 (2011) 3054–3059.
[9] C. Li, Y. Shi, N. Cai, J. Power Sources 196 (2011) 754–763.
[10] C. Li, Y. Shi, N. Cai, J. Power Sources 196 (2011) 4588–4593.
[11] C.G. Lee, H. Hur, M.B. Song, J. Electrochem. Soc. 158 (2011) B410–B415.
[12] M. LaBarbera, M. Fedkin, S. Lvov, ECS Trans. 35 (2011) 2725–2734.
[13] A. Kulkarni, S. Giddey, S.P.S. Badwal, Solid State Ionics 194 (2011) 46–52.
[14] L. Kouchachvili, M. Ikura, Int. J. Hydrogen Energy 36 (2011) 10263–10268.
[15] C. Jiang, J.T.S. Irvine, J. Power Sources 196 (2011) 7318–7322.
[16] P. Desclaux, S. Nürnberger, M. Rzepka, U. Stimming, Int. J. Hydrogen Energy 36 (2011) 10278–10281.
[17] Y. Bai, Y. Liu, Y. Tang, Y. Xie, J. Liu, Int. J. Hydrogen Energy 36 (2011) 9189–9194.
[18] H. Abernathy, R. Gemmen, K. Gerdes, M. Koslowske, T. Tao, J. Power Sources 196 (2011) 4564–4572.
[19] Y. Tang, J. Liu, Int. J. Hydrogen Energy 35 (2010) 11188–11193.
[20] S. Nurnberger, Bu, P. . Desclaux, B. Franke, M. Rzepka, U. Stimming, Energy Environ. Sci. 3 (2010) 150–153.
[21] R. Liu, C. Zhao, J. Li, F. Zeng, S. Wang, T. Wen, Z. Wen, J. Power Sources 195 (2010) 480–482.
[22] X. Li, Z. Zhu, R. De Marco, J. Bradley, A. Dicks, J. Power Sources 195 (2010) 4051–4058.
[23] H. Li, Q. Liu, Y. Li, Electrochim. Acta 55 (2010) 1958–1965.
[24] C. Li, Y. Shi, N. Cai, J. Power Sources 195 (2010) 4660–4666.
[25] J.-P. Kim, H. Lim, C.-H. Jeon, Y.-J. Chang, K.-N. Koh, S.-M. Choi, J.-H. Song, J. Power Sources 195 (2010) 7568–7573.
[26] L. Jia, Y. Tian, Q. Liu, C. Xia, J. Yu, Z. Wang, Y. Zhao, Y. Li, J. Power Sources 195 (2010) 5581–5586.
[27] A. Jayakumar, S. Lee, A. Hornes, J.M. Vohs, R.J. Gorte, J. Electrochem. Soc. 157 (2010) B365–B369.
[28] T.M. Gur, J. Electrochem. Soc. 157 (2010) B751–B759.
[29] M. Dudek, P. Tomczyk, Catal. Today 176 (2011) 388–392.
[30] M. Chen, C. Wang, X. Niu, S. Zhao, J. Tang, B. Zhu, Int. J. Hydrogen Energy 35 (2010) 2732–2736.
[31] D. Cao, G. Wang, C. Wang, J. Wang, T. Lu, Int. J. Hydrogen Energy 35 (2010) 1778–1782.
[32] Y. Wu, C. Su, C. Zhang, R. Ran, Z. Shao, Electrochem. Commun. 11 (2009) 1265–1268.
[33] Y. Nabae, K.D. Pointon, J.T.S. Irvine, J. Electrochem. Soc. 156 (2009) B716–B720.
[34] S.L. Jain, J. Barry Lakeman, K.D. Pointon, R. Marshall, J.T.S. Irvine, Energy Environ. Sci. 2 (2009) 687–693.
[35] X.Y. Zhao, Q. Yao, S.Q. Li, N.S. Cai, J. Power Sources 185 (2008) 104–111.
[36] H. Saito, S. Hasegawa, M. Ihara, J. Electrochem. Soc. 155 (2008) B443–B447.
[37] Y. Nabae, K.D. Pointon, J.T.S. Irvine, Energy Environ. Sci. 1 (2008) 148–155.
[38] Q. Liu, Y. Tian, C. Xia, L.T. Thompson, B. Liang, Y. Li, J. Power Sources 185 (2008) 1022–1029.
[39] X. Li, Z.H. Zhu, R.D. Marco, A. Dicks, J. Bradley, S. Liu, G.Q. Lu, Ind. Eng. Chem. Res. 47 (2008) 9670–9677.
[40] S. Li, A.C. Lee, R.E. Mitchell, T.M. Gür, Solid State Ionics 179 (2008) 1549–1552.
[41] A.C. Lee, S. Li, R.E. Mitchell, T.M. Gur, Electrochem. Solid-State Lett. 11 (2008) B20–B23.
[42] S.L. Jain, Y. Nabae, B.J. Lakeman, K.D. Pointon, J.T.S. Irvine, Solid State Ionics 179 (2008) 1417–1421.
[43] T. Tao, L. Bateman, J. Bentley, M. Slaney, ECS Trans. 5 (2007) 463–472.
[44] G.A. Hackett, J.W. Zondlo, R. Svensson, J. Power Sources 168 (2007) 111–118.
[45] K. Pointon, B. Lakeman, J. Irvine, J. Bradley, S. Jain, J. Power Sources 162 (2006) 750–756.
[46] S.J. Robert, J. Power Sources 160 (2006) 852–857.
[47] S. Zecevic, E.M. Patton, P. Parhami, Chem. Eng. Commun. 192 (2005) 1655–1670.
[48] N.J. Cherepy, R. Krueger, K.J. Fiet, A.F. Jankowski, J.F. Cooper, J. Electrochem. Soc. 152 (2005) A80–A87.
[49] S. Zecevic, E.M. Patton, P. Parhami, Carbon 42 (2004) 1983–1993.
[50] A. Jayakumar, R. Kungas, S. Roy, A. Javadekar, D.J. Buttrey, J.M. Vohs, R.J. Gorte, Energy Environ. Sci. 4 (2011) 4133–4137.
[51] W.H.A. Peelen, M. Olivry, S.F. Au, J.D. Fehribach, K. Hemmes, J. Appl. Electrochem 30 (2000) 1389–1395.
[52] X. Li, Z. Zhu, J. Chen, R. De Marco, A. Dicks, J. Bradley, G. Lu, J. Power Sources 186 (2009) 1–9.
[53] X. Li, Z. Zhu, R. De Marco, J. Bradley, A. Dicks, J. Phys. Chem. A 114 (2009) 3855–3862.
[54] J. Zhang, Z. Zhong, D. Shen, J. Zhao, H. Zhang, M. Yang, W. Li, Energy Fuels 25 (2011) 2187–2193.
[55] J.P. Paraknowitsch, A. Thomas, M. Antonietti, Chem. Mater. 21 (2009) 1170–1172.
[56] X. Li, Z. Zhu, R.D. Marco, J. Bradley, A. Dicks, Energy Fuels 23 (2009) 3721–3731.
[57] L. Qingfeng, F. Borup, I. Petrushina, N.J. Bjerrum, J. Electrochem. Soc. 146 (1999) 2449–2454.
[58] M.L. Orfield, D.A. Shores, J. Electrochem. Soc. 136 (1989) 2862–2866.
[59] K. Hemmes, M. Cassir, J. Fuel Cell Sci. Technol. 8 (2011) 051005.

[60] V.E. Hauser, in: Oregon State University, 1964.
[61] Y. Zhang, Inorg. Chem. 21 (1982) 3886–3889.
[62] J. Portier, G. Campet, J. Etourneau, B. Tanguy, J. Alloys Compd 209 (1994) 285–289.
[63] D.B. Weibel, R. Boulatov, A. Lee, R. Ferrigno, G.M. Whitesides, Angew. Chem. Int. Ed. 44 (2005) 5682–5686.
[64] A. Javadekar, A. Jayakumar, R.J. Gorte, J.M. Vohs, D.J. Buttrey, J. Electrochem. Soc. 158 (2011) B1472–B1478.
[65] S. Licht, B. Wang, Chem. Commun. 46 (2010) 7004–7006.
[66] H. Yin, D. Tang, H. Zhu, Y. Zhang, D. Wang, Electrochem. Commun. 13 (2011) 1521–1524.